Available online at www.sciencedirect.com
ScienceDirect
Journal of Hazardous Materials 140 (2007) 412–428
Journal of Hazardous Materials
www.elsevier.com/locate/jhazmat

Review

# Lessons learned from LNG safety research

Ronald P. Koopman [a,b,*], Donald L. Ermak [b]

[a] *Hazard Analysis Consulting, 4673 Almond Circle, Livermore, CA 94550, United States*
[b] *Lawrence Livermore National Laboratory, United States*

Available online 20 October 2006

**Abstract**

During the period from 1977 to 1989, the Lawrence Livermore National Laboratory (LLNL) conducted a liquefied gaseous fuels spill effects program under the sponsorship of the US Department of Energy, Department of Transportation, Gas Research Institute and others. The goal of this program was to develop and validate tools that could be used to predict the effects of a large liquefied gas spill through the execution of large scale field experiments and the development of computer models to make predictions for conditions under which tests could not be performed. Over the course of the program, three series of LNG spill experiments were performed to study cloud formation, dispersion, combustion and rapid phase transition (RPT) explosions.

The purpose of this paper is to provide an overview of this program, the lessons learned from 12 years of research as well as some recommendations for the future. The general conclusion from this program is that cold, dense gas related phenomena can dominate the dispersion of a large volume, high release rate spill of LNG especially under low ambient wind speed and stable atmospheric conditions, and therefore, it is necessary to include a detailed and validated description of these phenomena in computer models to adequately predict the consequences of a release.

Specific conclusions include:

- LNG vapor clouds are lower and wider than trace gas clouds and tend to follow the downhill slope of terrain due to dampened vertical turbulence and gravity flow within the cloud. Under low wind speed, stable atmospheric conditions, a bifurcated, two lobed structure develops.
- Navier–Stokes models provide the most complete description of LNG dispersion, while more highly parameterized Lagrangian models were found to be well suited to emergency response applications.
- The measured heat flux from LNG vapor cloud burns exceeded levels necessary for third degree burns and were large enough to ignite most flammable materials.
- RPTs are of two types, source generated and enrichment generated, and were observed to increase the burn area by a factor of two and to extend the downwind burn distance by 65%.

Additional large scale experiments and model development are recommended.


*Keywords:* LNG; Liquefied natural gas; Dense gas dispersion; Computer models; Lower flammability limit; Rapid phase transition explosion; Vapor cloud fire; Pool fire; Field experiments; Model validation

## Contents



* Corresponding author at: Hazard Analysis Consulting, 4673 Almond Circle, Livermore, CA 94550, United States. Tel.: +1 925 443 5324.
*E-mail address:* rpkoopman@comcast.net (R.P. Koopman).

0304-3894/$ – see front matter © 2006 Elsevier B.V. All rights reserved.
doi:10.1016/j.jhazmat.2006.10.042

## 1. Introduction

The goal of this paper is to summarize the lessons learned during more than a decade of research performed by Lawrence Livermore National Laboratory (LLNL) into the behavior of denser-than-air gases when released into the atmosphere. The LLNL research was conducted from 1977 to 1989 and was sponsored by the US Department of Energy (DOE), Department of Transportation (DOT), Gas Research Institute (GRI) and others. This paper is not intended to be a comprehensive review of all LNG research up to the present, although the authors have referenced prior and more current relevant work with which they are familiar.

LNG is one of the most difficult of the dense gases because it is initially intensely cold (−260 °F) and about 1.5 times the density of ambient air. As the cloud disperses, its density is affected by both mixing with the ambient air and heat transfer from the ground. If this vapor cloud is large enough, it will force the ambient air to flow over it, creating a shear layer that limits entrainment. Since the vapor cloud is denser than the surrounding air, it will be driven by gravity spreading flow out from the source and around obstacles with a tendency to follow the downhill slope of the terrain. The complexity of this behavior means that it is necessary to include a detailed description of the scientific phenomena driving the dispersion of the cold dense gas in order to be able to adequately predict the consequences of a release.

Research into LNG safety was initiated in the early 1970s by a number of Federal agencies with jurisdiction over various aspects of LNG importation and distribution. These included the US Coast Guard, Federal Railroad Administration, Maritime Administration, and Office of Pipeline Safety branches of the US Department of Transportation; the Federal Power Commission; the National Aeronautics and Space Administration (NASA); the US Bureau of Mines; and the Energy Research and Development Administration (ERDA), soon to become the US Department of Energy (DOE). In addition, significant research programs were underway in industry, including the American Gas Association LNG Safety Program and experimental work by Gaz de France, British Gas, Shell, and Esso. This work was summarized in a Report to Congress on Liquefied Energy Gas Safety by the Comptroller General of the US (GAO) in July 1978 (GAO Report) [1]. References to the many reports produced by these programs are provided in this report.

By 1977, primitive models developed by these projects were used to predict the dispersion distance to the lower flammable limit for the hypothetical instantaneous release of 25,000 $m^3$ of LNG from a ship. The results from six of these models varied from 0.75 to 50 miles [2]. This level of uncertainty resulted in the Federal Government initiating an LNG research program to put LNG accident prediction on a sound scientific footing in anticipation of the large scale importation of LNG and the public safety concerns surrounding LNG.

## 2. Phenomenology

Denser-than-air vapor clouds in the atmosphere are produced by a variety of mechanisms and conditions. Principally, this type of cloud is formed when the released vapor has a molecular weight greater than that of the ambient air or the released vapor is at a temperature that is sufficiently lower than the ambient temperature. In the case of LNG vapor which has a molecular weight of 16 versus approximately 28 for air, the denser-than-air cloud is due to the low temperature of the cryogenically stored LNG (about −160 °C). When LNG is released onto the ground or a water surface, it rapidly evaporates creating cold vapor that is about 1.5 times the density of ambient air. As the LNG vapor mixes with the ambient air, the LNG vapor temperature increases while the entrained air temperature decreases resulting in a denser-than-air vapor cloud mixture.

When a denser-than-air cloud is created at ground level several effects are observed in the dispersion of the denser-than-air cloud that are not observed in the dispersion of trace emissions. One is a reduction of vertical turbulent mixing with the ambient atmosphere due to stable density stratification of the dense gas cloud below the ambient atmosphere. Another is the generation of horizontal gravity-spreading flow due to density gradients in the horizontal direction. These two effects result in a lower and significantly wider cloud than is observed when a trace or neutrally buoyant gas is released. In some situations, the decoupling between the denser-than-air cloud and the ambient atmosphere is such that the dense gas cloud effectively displaces the ambient wind field [3–5] in much the same way that the wind flows over a solid body. This displacement results in a stably stratified dense gas layer and an interface through which it is difficult for external ambient turbulence to penetrate [6].

In addition to these dense gas dispersion effects, denser-than-air clouds often linger in the vicinity of the source region for extended periods of time, tend to follow the downhill slope independent of the ambient wind direction, and can become trapped or pool in valleys and low spots. A mitigating factor to all of these dense gas dispersion phenomena in the case of an LNG release is the heat flux from the ground or water surface into the cold LNG vapor cloud. The heat flux increases the temperature and decreases the density of the dense gas cloud, and can potentially lead to convective turbulence which increases mixing within the cloud.

All of these cold, dense gas dispersion effects have been observed experimentally [5,7–11]. Fig. 1 shows data from bivane anemometers both upwind and downwind of the 1980 Burro 8 LNG spill test at China Lake, CA. The wind speed recorded by the anemometer in the cloud drops to near zero when the cloud is present indicating that the cloud is displacing the ambient wind flow. Fig. 2 shows vertical turbulence data from a bivane anemometer as it experienced a cold dense LNG cloud during the 1987 Falcon 1 test. The reduction in the vertical turbulence level within the cold, dense gas LNG cloud is marked.

Gravity flow is driven by the excess hydrostatic pressure caused by the density difference between the cloud and the ambient atmosphere [6]. The fluid motion is generally horizontal except near the front where there is a recirculation vortex. Most of the mixing occurs just behind the front due to Kelvin–Helmholtz instability. For a continuous spill into a steady wind, gravity spreading also produces vortices in the crosswind direction which entrain air into the cloud at the edges.

Fig. 3 is a crosswind vertical cross section showing LNG concentration contours created by a FEM3 computer model simulation of the Burro 8 LNG test both with and without terrain compared to contours constructed from data [12]. Gravity flow in the crosswind direction produces the bifurcated and lobe structure. Terrain effects enhance the lobe on the left. Fig. 4 shows horizontal contours from the FEM3 computer simulation of Burro 8 with terrain effects compared to contours constructed from the data. The gravity-flow produced cloud bifurcation is even more apparent in this view.

Dense gas dispersion effects are most pronounced when the denser-than-air cloud is large, the ambient wind speed is low and the ambient atmospheric stability is stable [7]. As the cloud mixes with the surrounding ambient atmosphere, the cloud becomes more dilute, the in-cloud properties approach ambient levels, and the above mentioned effects begin to play a less significant role. Eventually, after the cloud has become much lower and wider than is observed from a neutrally buoyant release and after a considerable amount of dilution, the originally denser-than-air cloud begins to disperse like a trace gas cloud where dispersion is primarily controlled by the ambient wind speed and atmospheric stability.

All of these cold, dense gas dispersion phenomena – stable density stratification, reduced turbulence levels, gravity flow,

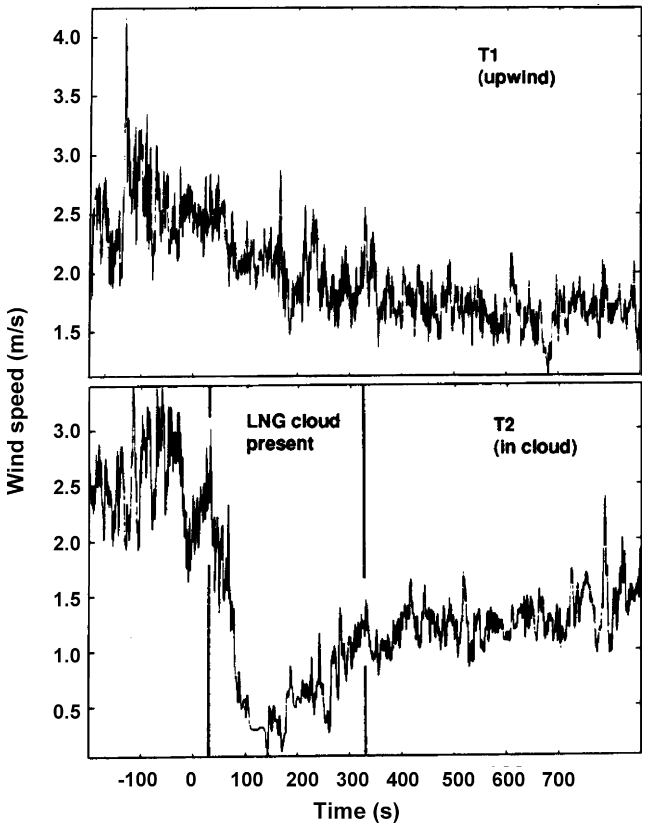


Fig. 1. Burro 8 anemometer data upwind and downwind of the spill point, showing significant modification of the wind speed due to the presence of the LNG cloud.

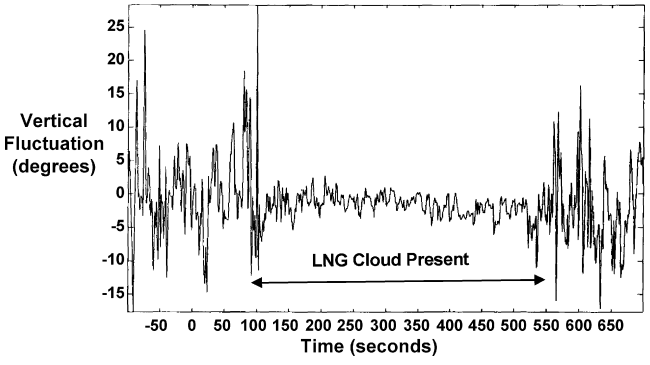


Fig. 2. Falcon 1 bivane anemometer data 150 m downwind of the vapor barrier showing the effect of the LNG vapor cloud on vertical fluctuations.

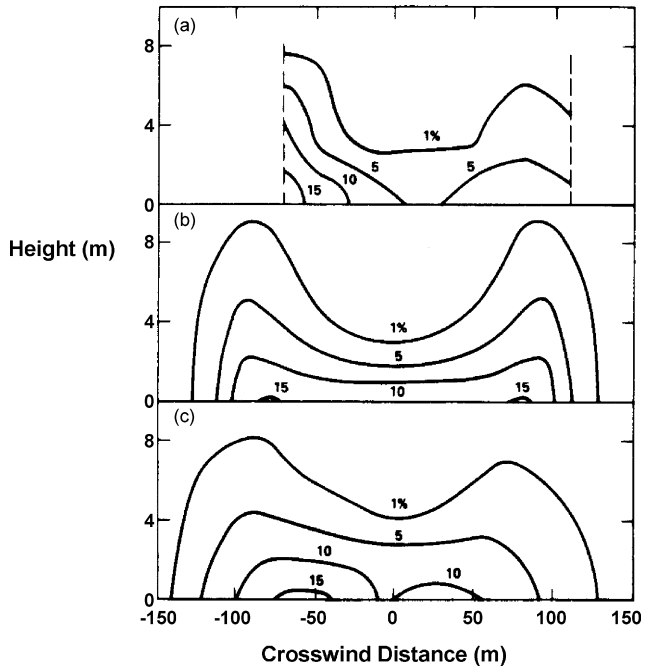


Fig. 3. Burro 8 crosswind vertical gas concentration contours at 140 m downwind and 180 s into the test (a), compared to FEM3 calculations with (c) and without China Lake terrain (b).

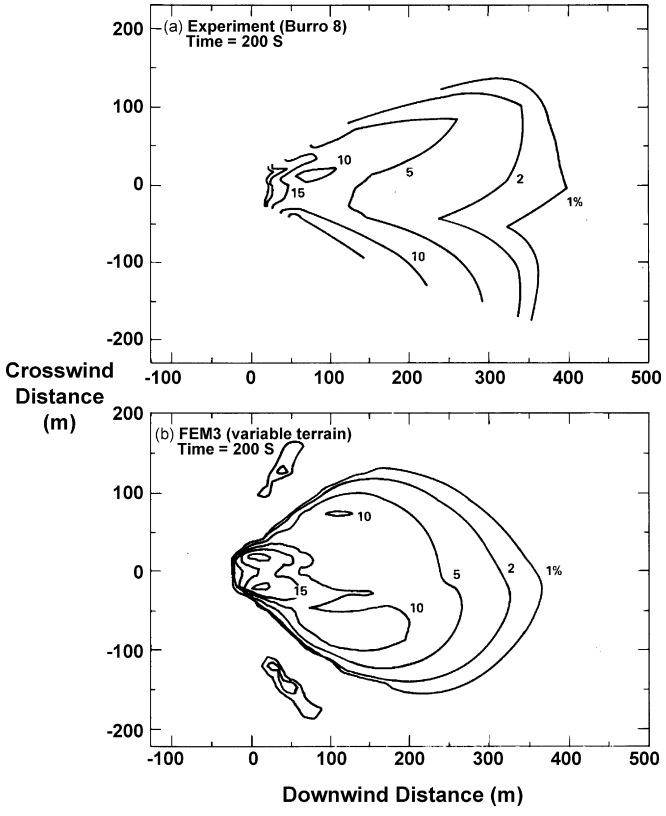


Fig. 4. Burro 8 horizontal gas concentration contours at 1 m elevation and 200 s into the spill (a) contours from field experiment data and (b) FEM3 calculation with China Lake terrain.

and ground heating of the cloud – along with the effects of terrain and obstacles, and other phenomena pertinent to the atmospheric dispersion of any substance, significantly influence the transport and dispersion of LNG vapor clouds and need to be included in computer models used to simulate the dispersion of an LNG release.

## 3. The experiments

### *3.1. Overview*

Experiments with LNG vapor production, dispersion and combustion have been conducted since the early 1970s, at lab scale and at field scale. For example, a number of pool fire and vapor cloud explosion tests were conducted at the Naval Weapons Center (NWC) in China Lake, CA. However, with the initiation of the US Department of Energy program, and with additional sponsorship by Gas Research Institute, larger and better instrumented field experiments were possible and were begun in 1978 by Lawrence Livermore National Laboratory (LLNL) and China Lake Naval Weapons Center (NWC) personnel with the Avocet series at the old Spill Test Facility. The China Lake facility was upgraded in the following year and in 1980 a much larger and better instrumented test series was conducted. It is interesting to note that simultaneously and completely independently, Shell Research conducted a series of LNG and LPG trials at Maplin Sands in England.

The 1980 China Lake LNG dispersion experiments consisted of eight LNG spill tests on water under a variety of meteorological conditions, know as the Burro series. These were followed in 1981 by 10 combustion, rapid phase transition (RPT) and dispersion tests, known as the Coyote series. Prior to Burro, Coyote and Maplin Sands, a number of pool fire, vapor burn and vapor cloud explosion tests were conducted at China Lake and are the subject of another paper.

After Burro and Coyote, DOE terminated its LNG research program and NWC closed its test facility. Other sponsors with interests in other hazardous gases came forward and the US Congress provided funds to construct a larger Spill Test Facility (STF) at the Nevada Test Site (NTS). In addition to the other hazardous materials of interest to these other industry and government sponsors, the US Department of Transportation and Gas Research Institute decided to sponsor an additional series of LNG tests to evaluate the effectiveness of a vapor containment fence or curtain. These tests were called the Falcon series and were conducted by LLNL at the newly constructed STF in 1987 [13].

The goal of all of these experiments was to measure the evaporation, dispersion and combustion of spilled LNG so intensively that the data sets produced could be used as benchmarks for the validation of computer models of that time and in the future. To do that required extensive measurements of meteorological parameters such as wind speed, temperature, turbulence, humidity, solar heat flux and gas cloud parameters such as concentration, temperature and ground heat flux, over an extensive area and at various heights. The intensive

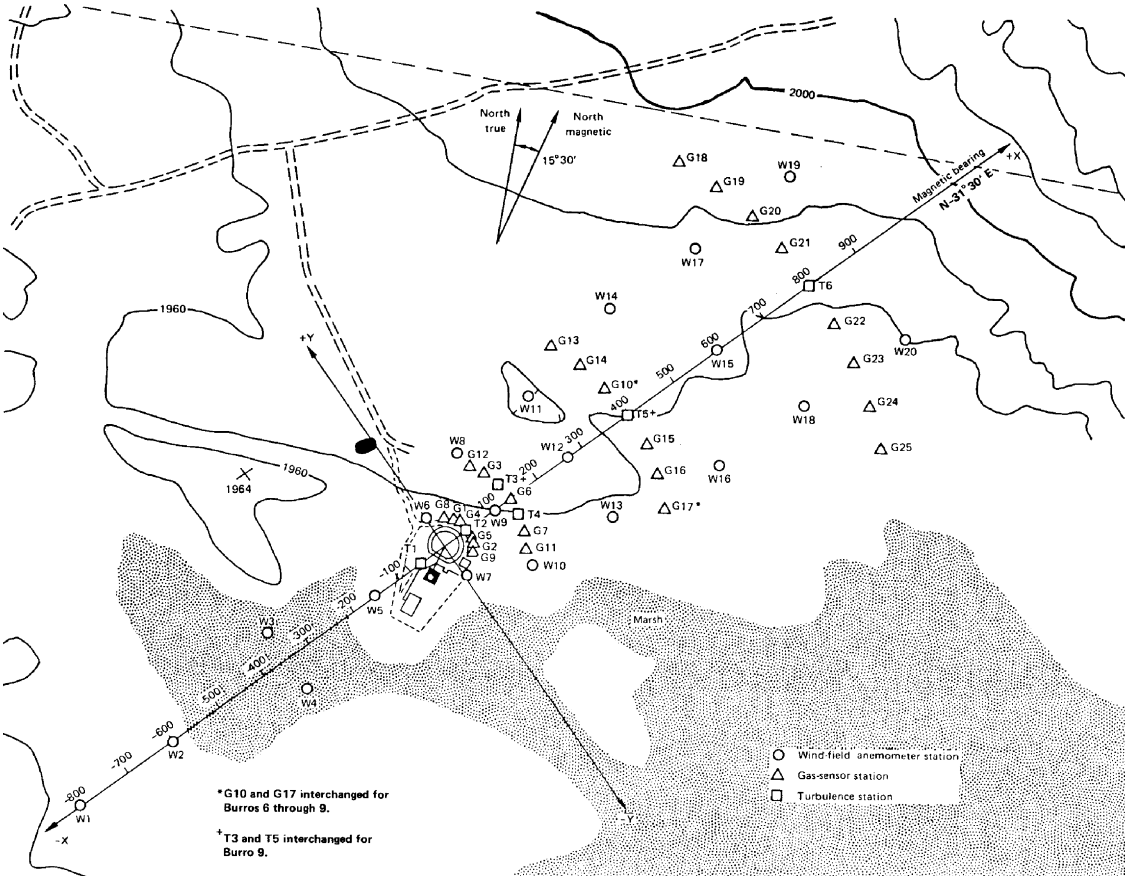


Fig. 5. Overhead view of the instrument array deployed for the Burro series.

instrument array used for the Burro series is shown in Fig. 5. It was necessary to conduct the tests under a variety meteorological and environmental conditions that would include all those that might be encountered in a real incident. This was an extremely ambitious undertaking. A summary of LNG tests and their characteristics is given in Table 1. Tests were also conducted with other hazardous materials, but only LNG tests will be covered in this report. From these tests, the best were selected to be benchmark tests for dispersion model validation [14]. These include: Burro 3, 7, 8, 9, Coyote 3, 5, 6, and Maplin (Shell) 15, 27, 29, 34, 35, 39, 56, with Falcon 1, 3, 4, added later.

### 3.2. Burro series tests

The main goal of the Burro series was to obtain extensive data on the dispersion of LNG vapor under a variety of meteorological conditions from spills on water. Of the eight Burro LNG tests conducted, four proved to be identifiably different from each other. These four were subjected to extensive analysis and are available in summary form for model validation [5,7,14,15].

Burro 3 was conducted under the most unstable atmospheric conditions encountered in the Burro series. The wind speed, 5.4 m/s, was in the midrange and the direction was steady such that the cloud went down the center of the array. Due principally

Table 1
Large scale LNG field tests

| Test | Date | Number | Size ($m^3$) | Rate ($m^3$/min) | Purpose |
|---|---|---|---|---|---|
| Avocet | 1978 | 4 | 4 | 3–5 | Dispersion |
| Maplin | 1980 | 13 | | 1–5 | Dispersion |
| | | 7 | 5–20 | Inst. | Combustion |
| Burro | 1980 | 8 | 24–39 | 12–18 | Dispersion |
| Coyote | 1981 | 5 | 3–14 | 6–19 | RPT |
| | | 5 | 8–28 | 14–17 | Dispersion/combustion |
| Falcon | 1987 | 5 | 20–66 | 9–30 | Dispersion from vapor fence |

to the unstable atmospheric conditions and in part to the low spill rate, the maximum distance to the LFL (5% by volume) was 180 m, the least of all the tests.

Burro 7 had the largest spill volume, 39.4 $m^3$, of all the Burro and Coyote tests and its spill duration of 174 s was among the longest. The wind speed, at 8.4 m/s was among the highest and the wind direction was such that part of the cloud extended beyond the right side of the array during most of the test. The atmospheric stability was slightly unstable. The centerline of the cloud remained within the array and it was possible to determine that the maximum distance to the LFL was 240 m. Because of the long duration of this spill, it provides a good example of steady state characteristics. When the vaporization rate equals the spill rate and the LFL has reached its furthest distance downwind, the vapor cloud is said to be in steady state. For this test, steady state existed for about 150 s at 140 m down wind, with concentrations varying from 3% to 7% during this time. According to analysis by Morgan et al. [7], this implies an uncertainty of about ±15% in concentration and also implies an uncertainty of ±15% in LFL distance.

Of all of the Burro and Coyote dispersion tests conducted, Burro 8 produced the most significant results. It was conducted with the highest ambient stability, (category E, slightly stable) and lowest wind speed (1.8 m/s) of all of the experiments. Consequently it experienced the least turbulence from the ambient atmosphere and its behavior was dominated by gravity flow and other internal cloud characteristics.

Burro 8 gave a glimpse of how very large LNG spills would dominate atmospheric dispersion. Turbulence within the cloud is dramatically reduced, producing the maximum LFL distance of all the tests, 445 m. Gravity flow led to the widest cloud for all the tests and produced a bifurcated cloud structure with strong influence of terrain on cloud shape which can be seen in Fig. 4. Here we see horizontal gas concentration contours constructed from the gas sensor data at 1 m above the ground and 200 s into the spill, compared to a FEM3 model calculation. Fig. 3 shows vertical concentration contours constructed from the gas sensor data at 140 m down wind and 180 s into the spill, compared to FEM3 calculations, both with and without terrain effects included. See Chan and Ermak [12], Chan et al. [16] and Ermak et al. [17] for more analysis of this test and comparison with models.

Because this cloud was so wide, meander had little effect on the gas concentration and we observed that ordinary atmospheric flow was excluded from the cloud, as can be seen in Fig. 1. Here we compare the wind speed immediately upwind of the release with that immediately downwind, in the cloud. The wind speed is dramatically reduced as the wind flows over the dense gas intrusion. Terrain effects become more important as gravity flow competes with wind driven flow. Because the wind speed was dropping during the test and because the ambient wind was virtually excluded by the dense cloud, the Burro 8 cloud persisted for a long time over the test area.

One other interesting result of this test is shown in Fig. 6, which shows a vertical contour of the cloud constructed from gas sensor data 400 m down wind and 400 s into the test. The highest gas concentration contour, 5%, is elevated above the 1 m level, showing evidence of slight buoyancy. This is in contrast

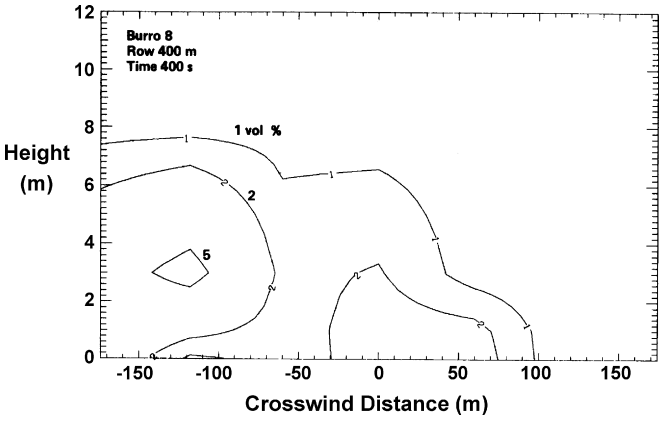


Fig. 6. Burro 8 vertical gas concentration contours at 400 m downwind and at 400 s into the spill.

to gas sensor data from other tests and up wind locations on this test which always show the highest concentrations at the lowest sensor, 1 m above the ground. A calculation of the cloud density based on concentration, temperature, and vapor composition gives a density of about 0.7% less than that of the surrounding air. This data indicate that if wind speeds are low enough and LNG vapor clouds linger long enough, they do show a small amount of buoyancy.

Because temperature is so important to LNG buoyancy, dispersion, and hazard distance, it is an important model validation parameter. Fig. 7 shows the measured temperature 140 m down wind compared to that calculated by FEM3, both with and without terrain effects included. Clearly terrain effects are important but do not account for all of the discrepancies between data and model. In Burro 8 the wind speed dropped continuously during the test and this is not taken into account by the model. Also not included in the model at the time of this calculation is ground cooling which reduces heat flow at late time.

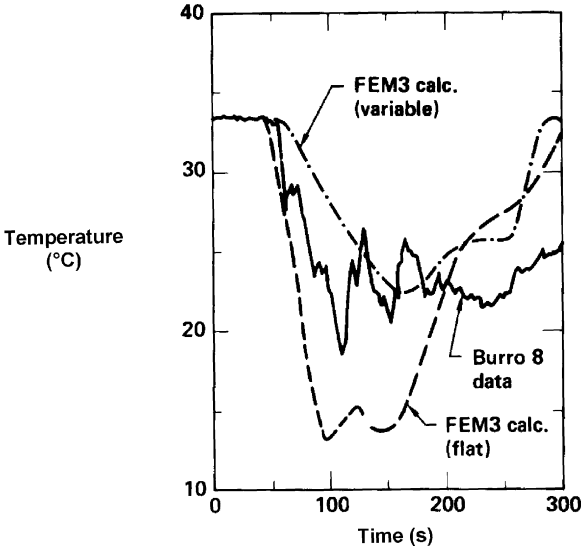


Fig. 7. Burro 8 temperature data compared to FEM3 calculations at 140 m down wind.

Burro 9 had the highest spill rate of any of the Burro or Coyote tests, 18.4 $m^3$/min. The wind speed was 5.7 m/s and the atmospheric stability was neutral (class D). The largest RPTs observed during the Burro and Coyote series occurred on this test, damaging the Spill Test Facility. See the report by McRae et al. [18] for more on the RPTs from both the Burro and Coyote series. Good quality data were obtained on this test and it should be considered a benchmark. It is relatively easy to separate out the RPT effects from the ordinary dispersion effects, but it should be noted that RPTs increased the LFL distance from a nominal 270 m to 410 m for brief periods of time. It is believed that the explosive force and shock wave from the RPT throws LNG into the air and turns it into aerosol and vapor, creating an LNG rich puff that propagates downwind.

### 3.3. Coyote series tests

#### 3.3.1. Coyote test summary

The Coyote series was conducted by LLNL in 1981 to explore systematically the large and damaging RPTs observed during the Burro series, to measure the characteristics of large vapor cloud fires, including the effect of high energy ignition sources and the potential for flame acceleration and the generation of damaging overpressure, and to obtain more dispersion data. Coyote 1, 4, 8, 9, and 10 were performed for RPT study and generally involved a succession of three short spill tests at different spill rates. Coyote 2, 3, 5, 6, and 7 were done for vapor burn study and also allowed the collection of dispersion data during most of the test. From these, Coyote 3, 5, and 6 were selected as benchmarks for dispersion model validation. The instrument array used was similar to that used for Burro 8 (see Fig. 5) but with the addition of IR imaging, heat flux calorimeters, flame speed devices, and radiometers. The Coyote test series is well documented by Goldwire et al. [19], Rodean et al. [20], McRae et al. [18] and Morgan et al. [7].

#### 3.3.2. Coyote dispersion and vapor burn tests

Coyote 3 occurred under the most unstable conditions of all of the Burro and Coyote tests, with an average wind speed of 6.0 m/s and category B–C stability. The spill volume was 14.6 $m^3$ and the spill rate was 13.5 $m^3$/min. The maximum distance to the LFL was about 195 m, one of the lowest of all the tests. Coyote 3 was ignited at 99.7 s. Fig. 8 shows a side view of the vapor burn in progress. The tall flame front on the left is moving downwind, while on the right, the flame front has moved back to the pool. Ignition occurred between the two visible flames. The nearly invisible hot gas ahead of, above, and behind the visible flame on the left, defines the burn area by an index of refraction change that can be seen by looking closely at the photograph. During analysis of the horizontal fire spread on Coyote 3 it was necessary to use 2-s averaged gas concentration data rather than 10-s averaged data because the 10-s averaged data suggested there was significant burn outside of the 5% contour. The width of the burned area was only about half the width of the pre-ignition 5% contour suggesting that flammable gas was sucked into the fire as the flame front passed by. The downwind length of the burn zone was essentially the same as the pre-ignition 5% contour and the area burned was about 3200 $m^2$, about half of what would be expected from the pre-ignition 5% contour. The flame velocity was about 20 m/s in this test, compared to 6 m/s wind speed. This test produced good quality fire and dispersion data.

Fig. 8. Coyote 3 vapor burn.

The wind speed for Coyote 5, 9.7 m/s, was higher than for any other test in the Burro or Coyote series, and the atmospheric stability was slightly unstable (category C–D). The spill volume was the largest for the series, 28 $m^3$, and the rate was 17.1 $m^3$/min. The cloud went right down the instrument array centerline with an LFL distance of about 205 m. A large RPT occurred at 101 s into the test and was followed within a few seconds by one or two smaller RPTs (see Fig. 9). It was observed that the RPT created puffs of gas temporarily increasing the LFL distance by 60 m, which was about 30%. Late in the spill, the ethane concentration in the cloud rose from an initial concentration of 20% to about 35% by volume. The cloud was ignited at 132.7 s.

The RPTs considerably enlarged the burn area over what it would have been with out them. The burn extended downwind about 250 m and was 60 m wide. As a result of the RPTs, the burn area was about 12,000 $m^2$, substantially greater than that estimated without RPTs, and the fire extended 65% further downwind that it would have without RPTs. Because of the ethane concentration, the burn area extended beyond the 5% contour, but not to the 4% contour.

Fig. 9. Coyote RPT.

Coyote 6 had the lowest wind speed of any of the vapor burn experiments, 4.6 m/s, and the atmospheric stability was neutral (category D). The average spill rate was 16.7 $m^3$/min and the spill volume was 22.8 $m^3$. The visible LNG vapor cloud, corresponding to a concentration of 11%, was considerably wider than for Coyote 3 and 5 and extended downwind 160 m. It also showed some of the same bifurcated structure observed so clearly in Burro 8 and characteristic of shear flow over an object. The cloud was ignited at 108 s, 79 m downwind of the spill point and the fire extended to 210 m downwind. With this test also, the total burn area was wider than the 5% contour, but not as much wider as was the case with Coyote 5, which was influenced by RPTs. The total burn area was 16,250 $m^2$, much larger than the other tests, due primarily to the lower wind speed and neutral stability conditions.

When Coyote 7 was conducted, most of the gas concentration measurement array had been disassembled in preparation for the RPT tests, so no contour plots are available, but motion pictures and IR images were obtained. The wind speed was moderate at 6 m/s and the atmospheric stability was neutral. This was a release of almost pure liquid methane (99.5%), with an average spill rate of 14.1 $m^3$/min and a spill volume was 26 $m^3$. This test was ignited with a high energy jet igniter to see if ignition energy had a significant effect on flame speed in an unconfined vapor cloud. The initial rate of flame spread was faster than with any other test. The jet igniter appears to have a large effect in the first 50 m of flame propagation, even in the direction opposite to the jet, but no effect thereafter. Since no array of gas sensors was present downwind, it is hard to estimate the burn area, but from the IR imagery it is estimated to be about 12,500 $m^2$.

### 3.3.3. Coyote vapor burn results

The total burn area for Coyote 6 was 16,250 $m^2$, much larger than Coyote 3 at 3200 $m^2$, Coyote 5 at 12,250 $m^2$ (much increased by late RPTs) and Coyote 7 at approximately 12,000 $m^2$, due primarily to the wider cloud created by the lower wind speed and neutral stability conditions. Except for Coyote 3, pre-ignition contours provided an underestimate of the burn area, by as much as a factor of two for RPT impacted Coyote 5 and 1.6 for Coyote 6. FEM3 calculations underestimated the burn areas by 26% for RPT impacted Coyote 5, and only 8% for Coyote 6, probably because RPT and terrain effects were not included in the model calculation (see Rodean et al. [20]).

One of the goals of these tests was to examine the effect of ignition source energy on flame speed to determine if there was a potential for damaging overpressures due to flame acceleration. The best data for this analysis came from overhead IR imagery which was present on Coyote 6 and 7. On Coyote 7 a high energy flame jet igniter built from a corrugated pipe 1.22 m long and 0.46 m in diameter, filled with a propane/air mixture, and capable of producing a jet of flame with a speed of 100–200 m/s was used to ignite the cloud. Unfortunately it only worked on this 99.5% pure methane test so the effect on LNG vapor clouds with higher levels of ethane and propane is not known. On the other tests, ordinary highway flares were used. In summary, the results of the flame speed analysis are as follows:

- Flame velocities in the laboratory frame varied from more than 40 m/s to just above wind velocity and decreased as the distance from the igniter increased.
- The wind did not have a strong influence on flame speed, particularly at early times. Fuel burn velocities of 6–24 m/s are consistent with the data.
- No flame acceleration was observed with these tests.
- The jet igniter had some effect on the rate of flame propagation through the first 50 m of the vapor cloud but no effect thereafter.
- The Coyote vapor burns did not produce damaging overpressures. The pressures observed were only a few millibars, probably because the flames were decelerating, not accelerating.

Heat flux measurements were also made on the Coyote vapor burn tests, both inside and outside of the cloud. *Inside the cloud*, four-heat flux calorimeters were placed on four towers closest to the ignition point and 1 m above the ground, facing away from the igniter and downwind. On Coyote 5, maximum measurements from calorimeters engulfed in flame were 220, 189 and 340 kW/$m^2$. On Coyote 6, maxima of 165 and 153 kW/$m^2$ were recorded, and on Coyote 7, a maximum of 291 kW/$m^2$ was measured. The heat flux pulses were of short duration, with a full width at half maximum of less than 2 s. The thermal impulse from the measurements varied from 348 to 507 kJ/$m^2$. These levels exceed those necessary for third degree burns by a large factor and are likely lethal. They are also great enough to ignite most flammable materials and did so during the tests.

*Outside the cloud*, nine radiometers were positioned at two locations on one side of the array centerline. Four were wide angle and five were narrow angle radiometers. The purpose of these measurements was to determine the emissive power of an unconfined vapor cloud fire and to determine the heat flux as a function of distance. Unfortunately there were many problems with the instruments, resulting in usable data only from three narrow angle radiometers on Coyote 3. The result is a flame emissive power in the range of 220–280 kW/$m^2$, consistent with that measured by Raj et al. [21] earlier at $210 \pm 65$ kW/$m^2$. This also implies that most of the peak heat flux inside the cloud (153–340 kW/$m^2$) was due to thermal radiation rather than convection.

### 3.3.4. Coyote RPT tests

A total of 13 RPT spills within five tests were conducted at various times during July through November of 1981. The goal of the RPT tests was to understand the physics behind RPT explosions so that their severity in an accidental spill could be predicted. These tests involved measurement of LNG species concentration, temperature of the LNG and the water, and velocity of the LNG as it exits the spill pipe, so that a comparison with Jazayeri's lab scale data [22], where the shock overpressure showed a dependence on impact pressure, water temperature, and type of cryogen, could be made. This also required installing blast gauges both above and below water on the spill pond. The RPT instruments were operational throughout the Coyote test series, recording data from a total of 18 separate spills involv-

ing spill rates from 6 to 19.4 $m^3$/min, spill volumes from 3.3 to 22.8 $m^3$, spill plate depth below water from 2.5 to 36 cm to no spill plate, water temperatures from 30 to 10.6 °C, LNG impact pressures from 0.8 to 15 psia, and LNG methane compositions from 99.5% to 70%, including three spills of liquid nitrogen. Documentation of these tests and analysis is provided by Goldwire et al. [19] and McRae et al. [18].

### 3.3.5. Coyote RPT test results

The Coyote RPT analysis [18] also includes data from the Burro tests bringing the total number of spill tests up to 26. Many large and damaging RPTs occurred during the Falcon tests which are not included in the analysis. RPTs were found to be of two fundamentally different types, those that occurred at any time in the spill, at the spill point, and were correlated with spill rate and those that generally occurred late in the spill, out on the edge of the LNG pool, and were correlated with ethane/propane concentration. Many RPT explosions were measured and their sizes varied from the equivalent of 3.5 kg of TNT, on Burro 9, down to a few grams of TNT. The RPT size correlation with spill rate can be seen in Fig. 10 and provides the best correlation of all the variables examined. The data indicate an apparent threshold or abrupt increase in strength at a spill rate of about 17 $m^3$/min. Unfortunately this was near the limit for the China Lake facility so rates substantially higher could not be tested. LNG composition also plays a role since it determines the thermodynamic parameters of the LNG including the superheat limit temperature, which is key to the production of RPTs.

In the early 1970s, Enger and Hartman [23] conducted a thorough study of the correlation of LNG composition with the occurrence of RPTs and established a compositional envelope within which RPTs occurred and outside of which they did not. Fig. 11 shows that envelope, the Enger and Hartman data, and the data from the Coyote and Burro tests. Enger and Hartman showed that RPTs occurred only when LNG compositions were high in ethane/propane. They also state that no RPTs occurred for LNG compositions with more than 40% methane.

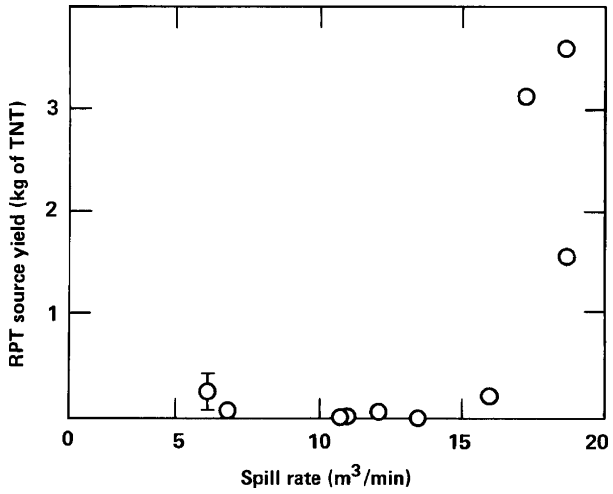


Fig. 10. The effect of spill rate on RPT size.

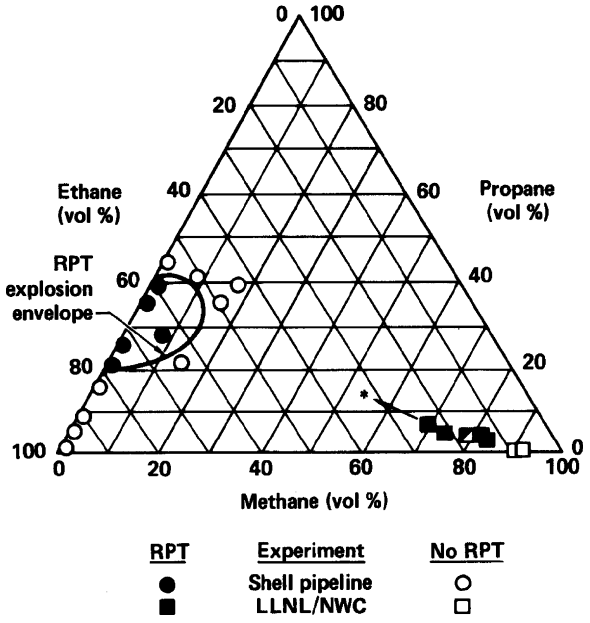


Fig. 11. Large scale RPTs and the Enger–Hartman RPT explosion envelope. The asterisk is an estimate of the maximum cool-down enrichment that could have occurred during the Coyote tests (on Coyote 2).

The China Lake RPTs are also shown in Fig. 11 and are clearly outside the Enger–Hartman envelope. Further, composition is not the only determining factor in the occurrence of RPTs, although it is important. The China Lake data show that large spill rates can produce RPTs even with initial methane compositions as high as 88%.

## 3.4. Falcon series tests

The objectives of the experiments were to provide a database of LNG dispersion data from large releases into a large vapor fence (44 m × 88 m × 8.7 m high) for comparison to wind tunnel models and mathematical models and to assess the effectiveness of vapor fences for mitigating LNG hazards in the event of an accidental spill. Five tests were conducted at the new Spill Test Facility (STF) at the Nevada Test Site (NTS), shown from overhead in Fig. 12. These were the largest spills so far, with release rates of 9–30 $m^3$/min and spill volumes ranging from 21 to 66 $m^3$. Three of these have been selected as validation benchmarks. The test series was terminated by an accidental ignition during the fifth test that damaged the test equipment. Data and test details may be found in the Falcon Data Report [13] and analysis and model/data comparison is provided by Chan [24].

Fig. 12. Overhead view of Spill Test Facility at NTS, showing two 100 $m^3$ cryogenic tanks, two 150 m long spill lines, and supporting equipment.

Falcon 1 had the highest spill volume, 66.4 $m^3$, and second highest spill rate, 28.7 $m^3$/min, and was conducted under very stable atmospheric conditions (category G with a wind speed of 1.7 m/s). The vapor cloud overflowed the vapor fence on all four sides in contrast to the pre-test wind tunnel simulation, which produced a vapor cloud essentially contained within the fence at all times [61]. A photograph of LNG vapor overflowing the fence during Falcon 1 is shown in Fig. 13.

Turbulence within the LNG vapor of Falcon 1 was significantly reduced, even in the cloud beyond the vapor fence. Damping of atmospheric turbulence downwind of this experiment is shown in Fig. 2. Here the vertical fluctuations of a bivane anemometer are greatly reduced when the cloud is present, indicating a reduction in mixing creating higher concentrations within the cloud and producing a longer LFL distance. Excellent data were obtained and because of the high spill rate and calm wind conditions, this test produced the most profound perturbation to the ambient wind field of all the Falcon tests and makes an excellent validation benchmark. Unfortunately Falcon 1 does not provide validation for free field dispersion from the full source, only from the vapor fence, which provided holdup and delay of a large amount of the vapor. Thus it cannot be easily used to validate the similarity profile models.

Falcon 2 had an intermediate spill rate (20.6 $m^3$ at 15.9 $m^3$/min), a short spill duration, 78 s, and was conducted under neutral atmospheric stability conditions. Unfortunately, much of the data were lost on this test.

Falcon 3 was also conducted under neutral conditions similar to Falcon 2, but more than twice as much was spilled over more than twice the duration (50.7 $m^3$ at 18.9 $m^3$/min) and good quality data were obtained. Fig. 14 shows gas concentration data from a sensor 150 m downwind of the vapor fence compared to a FEM3A model calculation [24]. The vapor fence and the environment inside were difficult to model, even with a sophisticated 3D computational fluid dynamics model like FEM3 and the good agreement between model calculation and data shown in this figure demonstrate considerable progress. RPTs occurred after about 60 s and caused some perturbation in the test data. Still, this test should be considered a benchmark.

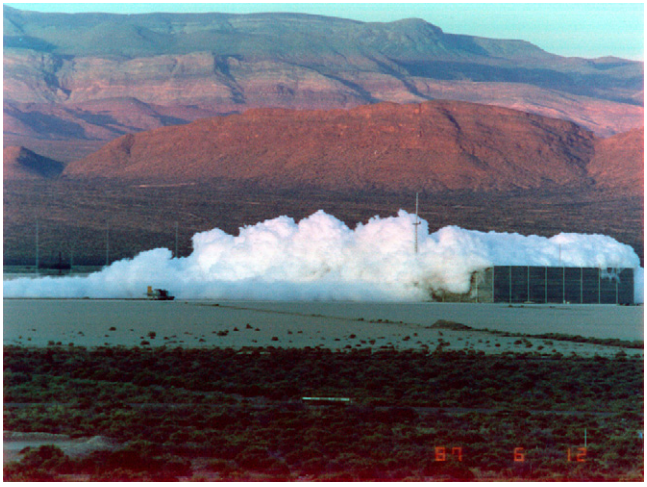

Fig. 13. Falcon 1 spill showing LNG vapor overflowing the vapor fence.

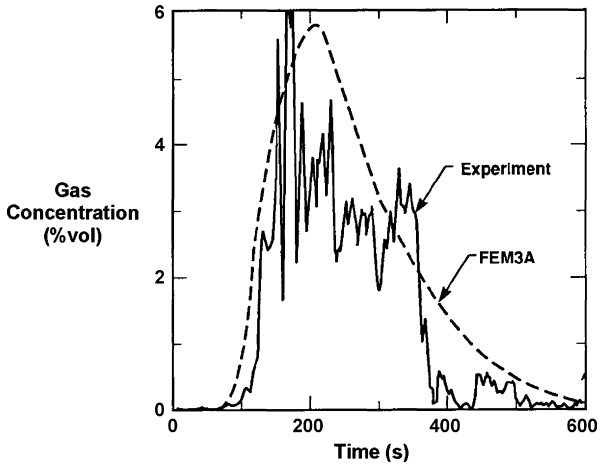


Fig. 14. Falcon 3 data 150 m downwind of vapor fence compared to FEM3A.

Falcon 4 had the smallest spill rate (44.9 $m^3$ spilled at 8.7 $m^3$/min) and longest spill duration (310 s) and was conducted under neutral to slightly stable atmospheric conditions. Because of the long spill duration, this test can be considered a continuous release during which all field variables reached steady state. This test should also be considered to be a benchmark.

Falcon 5 experienced large RPTs starting at about 60 s into the test, and an accidental ignition at about 81 s. As a result, data exist only for about 100 s for sensors downwind of the vapor fence.

## 4. Dispersion model development

### 4.1. Dense gas dispersion models

Numerical models of atmospheric dispersion differ in a variety of ways. Principal differences include the degree of completeness in the mathematical description of atmospheric dispersion processes, the type of releases (i.e. evaporating pool, jet, stack, explosion) that the model is capable of treating, the degree of completeness in the description of non-transport processes such as aerosol formation or chemical change, the type and completeness in the meteorological data and fields used to drive the dispersion model, and the complexity of terrain situations (with flat terrain being the simplest) for which the model is designed. Associated with these are the additional differences in numerical complexity and practical requirements of computer memory and speed.

During the 1980s, a number of models were developed to simulate the atmospheric dispersion of denser-than-air vapor clouds. These models essentially fell into three categories of varying physical completeness and numerical complexity: Navier–Stokes models, similarity-profile models and modified Gaussian models. There were several reviews of these models during this time [25–28] and more recently by Luketa-Hanlin [29]. Much of the information presented here was summarized from Ermak et al. [25].

The models which present the most physically complete description of dense gas dispersion are the Navier–Stokes mod-

els which are based on the three-dimensional, time-dependent conservation equations of mass, momentum, energy and species. Examples of this type of model are FEM3 [30], FEMSET [31], HEAVYGAS [32], and ZEPHYR [33], some of which may no longer be available. More recent examples include Fluent and CFX. CFX was recently used to reproduce the Coyote experiments [34,35]. These models were also evaluated in the recent scientific model evaluation of dense gas dispersion project, SMEDIS [36,37]. While these models provide the most complete description of the physical processes, they also require more computer power and time to run, compared to similarity models. At the intermediate level of completeness and complexity are the similarity profile models. These models use simplified forms of the conservation equations that are obtained by averaging the cloud properties over the crosswind plane or over the entire cloud. This generally reduces the mathematical complexity to one dimension. Quasi-three-dimensional solutions are obtained by using similarity profiles to regain the structure lost by averaging. Examples of this type of model are SLAB [38], HEGADAS [39], and DEGADIS [40]. At the simplest level are the modified Gaussian puff or plume models. These models are based on the Gaussian equation for the conservation of species and employ a variety of modifications to include the effects of dense gas dispersion within the Gaussian framework. Box or top-hat models, which are used to simulate instantaneous releases, fall into either the intermediate or simple category depending upon the complexity of the model with regard to the number of conservation equations to be solved.

The three types of models differ considerably in their approach to simulating the atmospheric dispersion of a dense gas release. Perhaps the most obvious differences are related to the degree to which each model type incorporates the basic conservation laws and three-dimensional, time-dependent effects. The modified Gaussian plume models are based on the single conservation of species equation and either neglect momentum and energy conservation or attempt to include them is some ad hoc manner. The intermediate similarity profile models include the conservation equations of mass, momentum, and energy, as well as species, but only in an average way. The Navier–Stokes models include the most complete description of the conservation laws by treating them explicitly in three-dimensions and time.

There are other important differences and these are related to the manner in which each model type treats the effects of gravity and turbulence. As previously noted, the modified Gaussian plume models use ad hoc formulas with empirical coefficients to describe the gravity spread and turbulent dispersion of the cloud. In contrast to this, the similarity profile and Navier–Stokes models use conservation principles to treat the effects of gravity. For example, this is done in the FEM3 Navier–Stokes model by solving the three momentum conservation equations including the buoyancy term and variable density, while the SLAB similarity profile model solves two layer-averaged momentum equations and uses the hydrostatic approximation.

With regard to turbulence, the similarity profile and Navier–Stokes models use different approaches. The similarity profile models use the concept of entrainment across the cloud–air interface and essentially neglect any explicit treatment of turbulence within the vapor cloud. Air is entrained into the cloud at the top and sides, and then is assumed to rapidly mix in the cloud creating a nearly uniform layer. Thus, there are two separate regions: the cloud and the ambient atmosphere. Mixing between the two is assumed to occur at the interface and is governed by an entrainment velocity which depends on the local properties of both the cloud and the surrounding atmosphere.

The Navier–Stokes models generally treat turbulence through the use of a turbulent diffusion coefficient or tensor that is determined using some form of turbulence closure. K-theory turbulence models have been used extensively in Navier–Stokes models (for example, FEM3 and ZEPHYR) for dense gas dispersion applications. These turbulence models assume local equilibrium and use a diffusion coefficient that depends on the local properties of the dense gas cloud and atmosphere. Higher order turbulence models, specifically k-epsilon models, have also been used. Higher order turbulence models do not assume local equilibrium and allow for the creation, transport and destruction of turbulence.

Three-dimensional, time-dependent Navier–Stokes models generally provide the most detailed and complete description of dense gas flow and dispersion within the atmosphere. These models are capable of simulating complex time-dependent phenomena and taking into account complex boundary conditions imposed by terrain and structures. However, this completeness and versatility comes at a price in the requirement for significant amounts of computer time, memory and power to run the models. To address this issue, a new category of dense gas dispersion models was developed in the 1990s that is between the Navier–Stokes and one-dimensional similarity profile models. Rather than developing entirely new models, efforts were focused on modifying existing models that were widely used in emergency response applications.

One popular approach to simulating the atmospheric dispersion of trace-gas releases under realistic conditions of terrain and time- and spatially-varying winds is to use a Lagrangian particle-in-cell, advection-diffusion model. In emergency response applications, realistic windfields based on timely meteorological data are input to the advection-diffusion model which simulates the dispersion of the release by calculating the trajectories of "marker particles". This approach has been shown to be well suited to operational uses for emergency response and accident preparedness purposes [41,42] because of the robustness and relatively high computational speed of the models on current day computers.

A dense gas version of the ADPIC particle-in-cell, advection-diffusion model [43] was developed by Ermak [44,45] by treating the dense gas effects as a perturbation to the ambient thermodynamic properties (density and temperature), ground level heat flux, turbulence level (diffusivity), and windfield (gravity flow) within the local region of the denser-than-air cloud. The perturbations are calculated from conservation of energy and momentum principles along with the ideal gas law equation of state for a mixture of gases. The various perturbations are expressed in terms of the vertically averaged thermodynamic and hydrodynamic properties of the cloud and

the local cloud height. Using a puff model rather than a particle-in-cell model, Sykes et al. [46] developed a dense gas version of the SCIPUFF Lagrangian puff dispersion model. In this case, dense gas effects were added by using the vorticity form of the momentum conservation equation.

An alternative approach to treating the effects of complex terrain on the flow of a dense gas cloud is to extend the one-dimensional similarity profile models to two spatial dimensions. Hankin and Britter [47,48] essentially used this approach in the development of the TWODEE shallow-layer model for the dispersion of dense gas releases. In this model, depth-averaged cloud properties are determined as a function of the two horizontal directions using the conservation laws and empirical correlations to determine the entrainment rate of air into the dense gas cloud. While the two-dimensional nature of this type of model allows for the treatment of dense gas flow over complex terrain, it also requires about an order of magnitude greater computational time than one-dimensional similarity profile models.

The dense gas dispersion models described above were developed using a variety of approaches with different levels of physical completeness and computer power requirements. In addition, these models were designed for and have been used for a variety of applications, including scientific research, safety assessment and emergency response guidance. Each of these applications has different requirements for accuracy, timeliness and computational cost. Of all the models, the Navier–Stokes models have the strongest scientific basis and provide the most detailed description of the flow and dispersion of a denser-than-air cloud in the atmosphere. Consequently, they are generally viewed as the best tool for scientific discovery in complex situations and for other applications that go beyond the limits of field validation.

### 4.2. Dispersion model validation

The authors of all the models described in the previous section have tested and verified their own models and have presented their results in numerous publications. For example, the FEM3 Navier–Stokes model and the SLAB similarity profile model have been extensively compared to the Burro, Coyote and Falcon LNG field experiments [7,24,49,50]. Similarly, the dense gas version of the ADPIC particle-in-cell model has been compared with the data from the Burro series experiments [45].

The 1984 [7] comparison of the FEM3 and SLAB models with the Burro and Coyote data was particularly detailed and included model-data comparisons of: LNG vapor concentration as a function of downwind distance, maximum distance to the lower flammability limit (LFL), crosswind distribution of LNG vapor concentration, horizontal distribution of LNG concentration, and LNG vapor cloud temperature and flow speed. In general, both models did well in predicting the properties of the Burro and Coyote LNG vapor clouds. They provided reasonable estimates of maximum LFL distance, and for the most part, they predicted the time dependence of concentration quite well. In addition, their predictions of cloud size and shape were also good. A particular achievement of the FEM3 model was the prediction of the bifurcated cloud structure observed in the Burro 8 experiment conducted under low ambient wind speed and stable atmospheric conditions.

Currently, FEM3 is the most well known Navier–Stokes model used in denser-than-air dispersion applications [29] and as previously noted, has been broadly evaluated. In addition to the model-data comparisons already cited, it has been evaluated for its ability to predict the flow and dispersion of a dense gas cloud over complex terrain [51], for the effectiveness of its turbulence submodel [52], and compared with the results of the Thorney Island Phase I trials [53]. The latest version, FEM3C [62,63], incorporates a phase change model that accounts for water vapor interaction in the cloud and includes an option to use a k-epsilon turbulence submodel. In addition, there is also an in-house massively parallel version of the model called FEM3-MP.

There have also been a number of model evaluation studies that were conducted by independent parties. Havens et al. [33] evaluated four Navier–Stokes models (FEM3, MARIAH, SIGMET-N and ZEPHYR) and found FEM3 and MARIAH to be the most suitable for dense gas dispersion applications. Two studies, one by TRC Environmental Corp. Inc. for the US Environmental Protection Agency [54] and the other by Sigma Research Corp. for the US Air Force and American Petroleum Institute [55] were performed to evaluate a number of models in the similarity profile and modified Gaussian categories of models. The TRC study evaluated seven models using data from three field experiments and found that all the models performed within a factor of 2. The Sigma Research study evaluated 15 hazardous gas models using data from eight field experiments and found that eight of the models produced relatively consistent predictions of plume centerline concentration across the dense gas data sets with relative mean bias of about ±30% or less and magnitudes of relative scatter that are about equal to the mean. More recently, the scientific model evaluation of dense gas dispersion project, SMEDIS, was commissioned by the European Union to develop a protocol and to evaluate dense gas dispersion models [36,37].

As new models are developed and applied to the atmospheric dispersion of large LNG vapor clouds, they too will need to be evaluated with data from LNG dispersion field experiments. Various approaches have been developed to evaluate atmospheric dispersion models and often the emphasis has been on the use of statistical methods. Sole reliance on statistical methods has been criticized by several authors [56,57] because these methods do not promote understanding of the underlying physical processes.

In 1988, Ermak [58] presented a methodology for evaluating dense gas dispersion models which relies heavily on physical understanding of the processes characteristic of dense gas releases in the atmosphere. Four plume parameters are recommended for comparison: maximum gas concentration, average ground-level plume centerline concentration, plume half-width and plume height, all as a function of downwind distance. The recommended comparison technique is based on ratios between the four model-predicted parameters and the experimentally observed values. Ratios allow comparison over a wide range of values from high concentrations where gravity spread effects

dominate down to trace concentration levels where ambient atmospheric phenomena dominate the flow and dispersion.

## 5. Lessons learned

The following conclusions are based on the analysis of experiments and model simulations conducted for LNG spills that were nominally 10–40 $m^3$ in size, at spill rates of 10–30 $m^3$/min, with a variety of meteorological conditions.

### 5.1. Dense gas dispersion phenomena

1. LNG spills form denser-than-air clouds that exhibit dense gas dispersion behavior. Two of the main effects are:

- Reduced vertical mixing with the ambient atmosphere and dampened vertical turbulence within the LNG vapor cloud due to stable density stratification.
- Gravity spreading flow due to density gradients in the horizontal plane between the dense gas cloud and the surrounding ambient atmosphere.

The above dense gas dispersion phenomena produce a lower and significantly wider cloud than is observed in clouds formed from neutrally buoyant or trace gas releases. Other related dense gas effects include: lingering of the cloud in the source region after the spill has ended, pooling in low spots and a tendency to follow the downhill slope in flow over terrain.

2. Under low wind speed, stable atmospheric conditions, the decoupling between the denser-than-air cloud and the ambient atmosphere can be such that the dense gas cloud effectively displaces the ambient wind field making it difficult for external ambient turbulence to penetrate the LNG vapor cloud (Burro 8). Under these conditions, the interaction between the ambient atmospheric flow and the gravity flow of the denser-than-air LNG vapor cloud produces two opposing vortices in the crosswind plane of the plume which causes it to bifurcate, forming a two lobed plume structure (as observed in Burro 8).
3. These dense gas effects increasingly dominate the dispersion of an LNG vapor cloud as spills become larger (spill volume and spill rate), the ambient wind speed becomes lower, and the atmosphere becomes more stable. The result is that low wind speed and a stable atmosphere create a worst case condition for the dispersion of an LNG vapor cloud, producing the largest flammable cloud with the furthest downwind distance to the LFL (Burro 8).
4. Heat transfer from the ground (or water) into the cold LNG vapor cloud increases cloud temperature and reduces cloud density, but generally not enough to make the cloud buoyant. If the wind speed is low enough and the atmosphere is stable enough, this heat transfer has been observed to create a slightly lighter-than-air LNG vapor cloud at large downwind distances (Burro 8).
5. All of these dense gas dispersion and heat transfer phenomena need to be included in atmospheric dispersion models used for predicting the dispersion of an LNG vapor cloud. Specifically, these include; variable temperature and density, an appropriate turbulence model for dense gas dispersion, an adequate ground-level heat transfer model, and gravity flow equations. Of course it is also necessary to include atmospheric stability, complex terrain, and source conditions. In order to reproduce field experiments for validation it may also be necessary to include time dependent wind speed and direction.

### 5.2. Dense gas dispersion models

Over the past three decades, numerous models have been developed and tested for their ability to predict the dispersion of a cold, dense gas cloud. These models fall into four categories of varying physical completeness and numerical complexity; Navier–Stokes models, modified Lagrangian puff or particle-in-cell models, similarity profile models and modified Gaussian or box models:

- The dense gas modified Lagrangian puff and particle-in-cell models are well suited to emergency response applications where time-limited simulations of cloud dispersion over realistic terrain with spatially- and time-varying winds are required.
- The Navier–Stokes models provide the most complete description of the flow and dispersion of a cold, denser-than-air cloud in the atmosphere and are well suited for research applications, dispersion simulations over complex terrain and obstacles, and other applications that go beyond the limits of field validation.

### 5.3. Vapor burns

Heat fluxes measured inside the vapor burns varied from 340 to 153 kW/$m^2$ with an average of 226 kW/$m^2$. The thermal impulse from the measurements varied from 348 to 507 kJ/$m^2$. These levels exceed those necessary for third degree burns by a large factor and are great enough to ignite most flammable materials.

### 5.4. RPTs

1. Two types of RPTs were observed:
   - Those that occurred at the spill point at any time during the spill and were correlated with spill rate.
   - Those that generally occurred out on the edge of the LNG pool late in the spill and were correlated with ethane/propane concentration.
2. The strength of RPTs was observed to vary from the equivalent of 3.5 kg of TNT down to a few grams of TNT.
3. Large spill rates can produce large RPTs even with initial methane compositions as high as 88%.
4. RPTs were observed to increase the burn area to two times that estimated without RPTs and to extend the downwind burn distance by 65% (Coyote 5). For spills on water, the consequences of RPTs on dispersion distances and burn areas

should be considered in the analysis. The puffs of LNG vapor created by the RPTs increase the hazard area significantly.

## 6. Looking to the future

### 6.1. Dispersion testing needed

All models, both physical and mathematical, contain approximations that limit their range of validity. To validate a model and establish its range of validity, we must be able to compare it with data over a significant portion of its expected range, including regions that exhibit all of the important phenomena. Since we have observed dense gas effects clearly dominating normal atmospheric dispersion phenomena only in Burro 8 and Falcon 1, and since Falcon 1 does not provide validation for free field dispersion from the full source, only from the vapor fence, this leaves only Burro 8 for free field model validation under low wind speed, stable atmospheric conditions. One test at one spill rate is not enough to have confidence that the models will adequately extrapolate to the much larger incidents of concern. We believe that additional dispersion experiments under stable atmospheric conditions and at larger spill rates and larger spill sizes are needed for model validation. The difficult question is how large do these tests need to be.

Since we endeavor to include all of the science needed to describe the atmospheric dispersion of LNG in the dispersion models and to base the models on the conservation laws of physics, it should not be necessary to perform full scale accident simulations. If properly constructed and validated, the models can be used to scale up to larger spills than those tested. Table 2 provides a summary of spill rates and sizes for the experiments to date, the maximum capability of the Spill Test Facility (STF) at NTS, and two full scale incident scenarios. The first incident is a ship collision under worst case conditions, puncturing both the outer and inner hulls of a LNG tanker ship and resulting in a 1–2 $m^2$ hole in a 25,000 $m^3$ LNG tank [59]. The LNG will flow out of the hole at an initial rate of about 1000 $m^3$/min and will continue at a decreasing rate until the tank has emptied to the top of the hole (approximately 12,500 $m^3$). The second incident is an attack on a ship using explosives, creating a 5 $m^2$ hole [59]. It is very likely that the explosives will ignite the LNG at the ship resulting in a large pool fire, not a dispersing cloud of LNG vapor.

The additional LNG spill tests needed for dispersion model validation under low wind speed, stable atmospheric conditions could be performed at the Nevada Test Site Spill Test Facility (also know as the Hazmat Spill Center and the Non-Proliferation Test and Evaluation Center). The full cryogenic capacity of the facility is 200 $m^3$ and the maximum spill rate is 100 $m^3$/min. This facility, with its two 100 $m^3$ cryogenic tanks, and two 150 m long spill lines (see Fig. 12), was designed and built in the mid 1980s for just this purpose. The spill rate in the worst case ship accident mentioned above is only 10 times the rate of the STF. Even though the total volume of the ship tank is over 100 times the capability of the STF, the most important parameter for dispersion is the spill rate, not the total volume. At a given spill rate and given atmospheric conditions, the vapor cloud produced by a spill will reach steady state a few minutes into the spill. This means that the downwind hazard distance or distance to the LFL, will not increase further (it will fluctuate) even though the spill may continue for some time. If the spill is long enough to achieve steady state, the total volume does not affect the hazard distance. The models, if properly validated and upgraded as needed, can be expected to accurately extrapolate up a factor of ten or more in spill rate.

Table 2
Potential incidents, past tests and the STF

| Incident | Spill rate ($m^3$/min) | Spill size ($m^3$) |
|---|---|---|
| Tests to date | 1–30 | 4–66 |
| Ship collision (1–2 $m^2$ hole) | 1000 | 12,500 |
| Attack on ship (5 $m^2$ hole) | 3000 | 12,500 |
| Spill Test Facility capability | 100 | 200 |

The testing mentioned above is important for model validation of releases on flat terrain or water. Large scale test data for releases on variable terrain and in an urban environment would also be very useful.

### 6.2. Dispersion model development needed

As previously noted, models used to simulate the dispersion of LNG vapor clouds need to include the physical phenomena associated with cold, denser-than-air vapor clouds and be properly validated with field scale data. Past experiments show that these phenomena include variable temperature and density, turbulence damping, ground level heating and gravity flow. Because of these, turbulence, which affects all of these phenomena, is generally considered to be the most difficult to treat properly [28,50].

For the Navier–Stokes models, higher order turbulence models, such as the widely used k-epsilon models, are a potential improvement (over K-theory models) because they do not assume local equilibrium and allow for the creation, transport and destruction of turbulence. Similarly, large eddy simulation models would be useful in estimating concentration fluctuations and peak concentration. However, these more advanced turbulence models must also include the effects associated with the dispersion of cold, denser-than-air vapor clouds. And in particular, they must be capable of adequately reproducing the turbulence damping and complicated bifurcated plume structure observed in Burro 8 and the lofted plume centerline observed at larger downwind distances also in Burro 8.

As these models are used to simulate larger and larger releases [58], it becomes necessary to consider if all of the relevant phenomena are included. Under worst case stable atmospheric conditions, the boundary layer is typically a few hundred meters high and the horizontal wind shear over this height is as much as 30° due to the interaction of the Coriolis force with the ambient vertical momentum flux [60]. To predict this wind shear and stable density and temperature structure, meteorological weather models include submodels for solar radiation, ther-

mal and water fluxes at the ground, cloud effects, and water as a separate species from air in addition to the Coriolis force within the basic conservation equations and an appropriate turbulence model. While these phenomena are generally included in Navier–Stokes meteorological models, they are currently not included in the Navier–Stokes dense gas models.

To evaluate the importance of these phenomena in the large LNG release scenarios under consideration, one could start by simulating these releases using current Navier–Stokes dense gas models and comparing the size of the model predicted LNG vapor clouds with the height of the stable boundary layer. This would provide an initial indication of the importance that the Coriolis force might have on the dispersion of large LNG vapor clouds. A second step would be to include the Coriolis force and other essential meteorological submodels in the dense gas Navier–Stokes model and repeat these scenario simulations. This would allow for a direct model comparison of the interaction of the Coriolis force with the gravity flow force (induced hydrostatic pressure) within the LNG vapor cloud.

In recent years, Navier–Stokes atmospheric dispersion models have been used to study trace gas dispersion in the urban environment around structures and buildings for detailed planning studies and to study meteorological coupling with larger scale models to provide more appropriate initial and boundary conditions for local scale dispersion models. The extension of this work to include large LNG releases would be appropriate for similar high risk scenarios. In addition, fast-running dense gas dispersion models that include parameterized cold, dense gas effects, complex terrain (mountains, valleys, etc.), and three-dimensional meteorology are needed for emergency response applications.

Even with these model improvements and enhancements, the models still contain approximations that limit their range of validity and this is where field validation experiments play an important role. The final step is to compare the model predictions with the data from any new experiments that are performed.

### 6.3. Additional combustion research needed

A recent review article [29] concluded that there is a shortage of data for large LNG pool fires on water. It was also pointed out in the same article that mass fire behavior may occur as the pool diameter increases beyond a certain diameter and the flame envelope breaks up into multiple fires, each having a smaller flame height. For distances greater than a pool diameter, the thermal radiation would be less for the mass fire than for the single coherent plume assumed in all current hazard analysis. This implies a potential reduction in thermal hazard distance for large fires of a factor of 2–3. Tests with pool diameters up to 100 m could be performed at the Spill Test Facility at NTS. These larger pool fire tests would determine the threshold for mass fire formation and the effect on surface emissive power, smoke shielding, view factor, and burn rate.

It has also been suggested that waves could have a significant effect on LNG vaporization and pool fires. No adequate model has yet been produced and no experimental data currently exist to guide or confirm model development in this area. Large scale LNG vaporization tests, on water with waves, ignited and unignited, could answer these questions.

### 6.4. Additional RPT tests needed

The Burro and Coyote tests established a correlation between spill rate and RPT size but they were limited by the China Lake facility to about 19 $m^3$/min. The onset of the large RPTs corresponded to a spill rate of about 17 $m^3$/min, very close to the limit of the China Lake facility. Thus experiments at higher rates to examine the correlation were not possible. Experiments with spill rates of up to 100 $m^3$/min can be conducted at the NTS Spill Test Facility and would allow evaluation of the correlation over a range of spill rates, possibly leading to determination of the maximum potential size of RPTs as well as providing more information on the mechanism creating large scale RPTs.

## References

[1] Report to the congress by the comptroller general of the United States, Liquefied Energy Gases Safety, three volumes, EMD-78-28, July 31, 1978.
[2] J. Havens, An assessment, United States Coast Guard report, CG-M-09-77, April 1977.
[3] R.P. Koopman, Atmospheric dispersion of large-scale spills, in: Proceedings of the AICHE Symposium Series, 1986, Cryo. Prop. Process. Appl. 82 (251) (1987) 141–159.
[4] R.P. Koopman, D.L. Ermak, S.T. Chan, A review of recent field tests and mathematical modeling of atmospheric dispersion of large spills of denser-than-air gases, Atmos. Environ.23 (4) (1989) 731–745.
[5] R.P. Koopman, R.T. Cederwall, D.L. Ermak, H.C. Goldwire, W.J. Hogan, J.W. McClure, T.G. McRae, D.L. Morgan, H.C. Rodean, J.H. Shinn, Analysis of Burro series 40-$m^3$ LNG spill experiments, J. Hazard. Mater. 6 (1/2) (1982) 43–83.
[6] J.C.R. Hunt, J.W. Rothman, R.E. Britter, Some physical processes involved in the dispersion of dense gases, in: IUTAM Symposium on Atmospheric Dispersion of Heavy Gases and Small Particles, Delft, The Netherlands, August, 1983.
[7] D.L. Morgan, L.K. Morris, S.T. Chan, D.L. Ermak, T.G. McRae, R.T. Cederwall, R.P. Koopman, H.C. Goldwire, J.W. McClure, W.J. Hogan, Phenomenology and modeling of liquefied natural gas vapor, Lawrence Livermore National Laboratory, UCRL-53581, April 1984.
[8] S.J. Wiersma, T.A. Williams, Overview of LNG vapor dispersion research, in: International Conference on Liquefied Natural Gas, vol. 2, 9th ed., Nice, France, October 17–20, 1989.
[9] J.S. Puttock, D.R. Blackmore, G.W. Colenbrander, Field experiments on dense gas dispersion, J. Hazard. Mater. 6 (1982) 13–41.
[10] D.R. Blackmore, J.A. Eyre, G.G. Summers, Dispersion and combustion behavior of gas clouds resulting from large spillages of LNG and LPG on to the sea, Trans. I. Mar. E.$^{TM}$ 94, paper 29, 1982.
[11] G.W. Colenbrander, J.S. Puttock, Dense gas dispersion behavior, experimental observations and model development, in: Proceedings of the Fourth International Symposium on Loss Prevention and Safety, vol. 90, 1983, pp. F66–F76.
[12] S.T. Chan, D.L. Ermak, Recent results in simulating LNG vapor dispersion over variable terrain, in: Proceedings of the IUTAM Symposium on Atmospheric Dispersion of Heavy Gases and Small Particles, Delft University of Technology, The Netherlands, August 29–September 2, 1983, 1983 (see also Lawrence Livermore National Laboratory, UCRL-88495 Rev. 1).
[13] T.C. Brown, et al., Falcon Series Data Report, 1987. LNG Vapor Barrier Verification Field Trials, Lawrence Livermore National Laboratory, UCRL-CR-104316, June 1990.

[14] D.L. Ermak, R. Chapman, H.C. Goldwire, F.J. Gouveia, H.C. Rodean, Heavy Gas Dispersion Test Summary Report, Lawrence Livermore National Laboratory, UCRL-21210, October 1988.
[15] R.P. Koopman, et al., Burro Series Data Report LLNL/NWC 1980 LNG Spill Tests, UCID-19075, Lawrence Livermore National Laboratory, 1982.
[16] S.T. Chan, H.C. Rodean, D.L. Ermak, Numerical simulation of atmospheric releases of heavy gases over variable terrain Air Pollution Modeling and Its Applications III, vol. 5, Plenum Press, New York, 1984, pp. 295–328.
[17] D.L. Ermak, S.T. Chan, D.L. Morgan, L.K. Morris, A comparison of dense gas dispersion simulations with the Burro series LNG spill test results, J. Hazard. Mater. 6 (1/2) (1982) 129–160.
[18] T.G. McRae, H.C. Goldwire Jr., R.P. Koopman, Analysis of Large-Scale LNG/Water RPT Explosions, Lawrence Livermore National Laboratory, Livermore, CA, 1984 (UCRL 91832).
[19] H.C. Goldwire Jr., H.C. Rodean, R.T. Cederwall, E.J. Kansa, R.P. Koopman, J.W. McClure, T.G. McRae, L.K. Morris, L. Kamppinen, R.D. Kiefer, Coyote Series Data Report, LLNL/NWC 1981 LNG Spill Tests Dispersion, Vapor Burn, and Rapid-Phase-Transition, UCID-19953, vols. 1/2, October 1983.
[20] H.C. Rodean, W.J. Hogan, P.A. Urtiew, H.C. Goldwire Jr., T.G. McRae, D.L. Morgan Jr., Vapor Burn Analysis for the Coyote Series LNG Spill Experiments, Lawrence Livermore National Laboratory, 1984 (UCRL-53530).
[21] P.K. Raj, A.N. Moussa, K. Aravamudan, Experiments involving pool and vapor fires from spills of liquefied natural gas on water, US Department of Transportation Report no. CG-D-55-79 (ADA077073), 1979.
[22] B. Jazayeri, Impact cryogenic vapor explosions, MS Thesis, Massachusetts Institute of Technology, Cambridge, MA, 1975.
[23] T. Enger, D.E. Hartman, LNG Spillage on Water, Shell Pipeline Corp., Technical Progress Report 1-72, February 1972.
[24] S.T. Chan, Numerical simulations of LNG vapor dispersion from a fenced storage area, J. Hazard. Mater. 30 (1992) 195–224.
[25] D.L. Ermak, H.C. Rodean, R. Lang, S.T. Chan, A Survey of Denser-than-air Atmospheric Dispersion Models, Lawrence Livermore National Laboratory, Livermore, CA, 1988 (UCRL-21024).
[26] D.R. Blackmore, M.N. Herman, J.L. Woodward, Heavy gas dispersion models, J. Hazard. Mater. 6 (1982) 106–128.
[27] J.A. Havens, A review of mathematical models for prediction of heavy gas atmospheric dispersion, J. Chem. E. Symp. Ser. 71 (1982).
[28] C.J. Wheatley, D.M. Webber, Aspects of the dispersion of denser-than-air vapours relevant to gas cloud explosions, Contract Report SR/007/80/UK/H/-EAEC/UKAEA No. XII/829/84-EN, 1984.
[29] A. Luketa-Hanlin, R. Koopman, D. Ermak, On the application of computational fluid dynamics codes for liquefied natural gas dispersion, J. Hazard. Mater. 140 (2007) 504–517.
[30] S.T. Chan, FEM3-A Finite Element Model for the Simulation of Gas Transport and Dispersion: User's Manual, UCRL-21043, Lawrence Livermore National Laboratory, Livermore, CA, 1988.
[31] P.L. Betts, V. Harountunian, Finite element calculations of transient dense-gas-dispersion, in: Proceedings of the IMA Conference on Stably Stratified Flows and Dense Gas Dispersion, Chester, England, 1986.
[32] D.M. Deaves, Application of advanced turbulence models in determining the structure and dispersion of heavy-gas clouds, in: G. Ooms, H. Tenneckes (Eds.), Atmospheric Dispersion of Heavy Gases and Small Particles, Springer-Verlag, Berlin, Germany, 1984.
[33] J.A. Havens, P.J. Schreurs, T.O. Spicer, Evaluation of 3D hydrodynamic computer models for prediction of LNG vapor dispersion in the atmosphere, Final Report to the Gas Research Institute, Chicago, Illinois, 1986.
[34] S. Sklavounos, F. Rigas, Simulation of the Coyote series trials. Part I: CFD estimation of non-isothermal LNG releases and comparison with box-model predictions, Chem. Eng. Sci. 61 (2006) 1434–1443.
[35] F. Rigas, S. Sklavounos, Simulation of the Coyote series trials. Part II: A computational approach to ignition and combustion of flammable vapor clouds, Chem. Eng. Sci. 61 (2006) 1444–1452.
[36] N.C. Daish, R.E. Britter, P.F. Linden, S.F. Jagger, B. Carissimo, SMEDIS: Scientific model evaluation of dense gas dispersion models, Int. J. Environ. Pollut. 14 (1–6) (2000).
[37] B. Carissimo, S.F. Jagger, N.C. Daish, A. Halford, S. Selmer-Olsen, K. Riikonen, J.M. Perroux, J. Wurtz, J.G. Bartzis, N.J. Duijm, K. Ham, M. Schatzmann, R. Hall, The SMEDIS database and validation exercise, Int. J. Environ. Pollut. 16 (1–6) (2001).
[38] D.L. Ermak, User's Manual for SLAB: An Atmospheric Dispersion Model for Denser-than-air Releases, UCRL-MA-105604, Lawrence Livermore National Laboratory, Livermore, CA, 1990.
[39] G.W. Colenbrander, A mathematical model for the transient behavior of dense vapor clouds, in: Proceedings of the Third International Symposium on Loss Prevention and Safety Promotion in the Process Industries, Basle, Switzerland, 1980.
[40] T.O. Spicer, J.A. Havens, Development of a heavier-than-air dispersion model for the US Coast Guard Hazard Assessment Computer System, in: S. Hartwig (Ed.), Heavy Gas Risk Assessment III, Reidel, Dortrecht, The Netherlands, 1986.
[41] M.H. Dickerson, R.C. Orphan, Atmospheric release advisory capability, Nucl. Safe. 17 (1976) 281.
[42] T.J. Sullivan, S.S. Taylor, A computerized radiological emergency response and assessment system, in: Proceedings of an International Symposium on Emergency Planning and Preparedness for Nuclear Facilities, International Atomic Energy Agency, Rome, Italy, November 4–8, 1985.
[43] R. Lange, A Three-dimensional particle-in-cell model for the dispersal of atmospheric pollutants and its comparison to regional tracer studies, J. Appl. Meteorol. 17 (1978) 320.
[44] D.L. Ermak, A concept for treating dense-gas dispersion under realistic conditions of terrain and variable winds, in: Proceedings of the JANNAF Safety and Environmental Protection Subcommittee Meeting, Livermore, CA, June 18–22, 1990.
[45] D.L. Ermak, Dense-gas dispersion advection-diffusion model, in: Proceedings of the JANNAF Safety and Environmental Protection Subcommittee Meeting, Monterey, CA, August 10–14, 1992.
[46] R.I. Sykes, C.P. Cerasoli, D.S. Henn, The representation of dynamic flow effects in a Lagrangian puff dispersion model, J. Hazard. Mater. 64 (1999) 223–247.
[47] R.K.S. Hankin, R.E. Britter, TWODEE: the health and safety laboratory's shallow layer model for heavy gas dispersion. Part I: Mathematical basis and physical assumptions, J. Hazard. Mater. 66 (1999) 211–226.
[48] R.K.S. Hankin, Heavy gas dispersion: integral models and shallow layer models, J. Hazard. Mater. 102 (2003) 1–10.
[49] D.L. Ermak, S.T. Chan, D.L. Morgan, L.K. Morris, A comparison of dense gas dispersion model simulations with burro series LNG spill test results, J. Hazard. Mater. 6 (1982) 129–160.
[50] D.L. Ermak, S.T. Chan, A study of heavy gas effects on the atmospheric dispersion of dense gases, in: C. De Wispelaere, F.A. Schiermeier, N.V. Gillani (Eds.), Air Pollution Modeling and Its Applications, Plenum Press, New York, 1986.
[51] S.T. Chan, D.L. Ermak, Further assessment of FEM3—a numerical model for the dispersion of heavy gases over complex terrain, in: Proceedings of the JANNAF Safety and Environmental Protection Subcommittee Meeting, Monterey, CA, November 4–8, 1985.
[52] D.L. Ermak, S.T. Chan, FEM3 Dispersion Calculations: Evaluation of Turbulence Submodel, UCID-20933, Lawrence Livermore National Laboratory, Livermore, CA, 1986.
[53] S.T. Chan, D.L. Ermak, L.K. Morris, FEM3 model simulations of selected Thorney Island phase I trials, J. Hazard. Mater. 16 (1987) 267.
[54] J.S. Touma, W.M. Cox, H. Thistle, J.G. Zapert, Performance evaluation of dense gas dispersion models, J. Appl. Meteorol. 34 (1995) 603–615.
[55] S.R. Hanna, J.C. Chang, D.G. Strimaitis, Hazardous gas model evaluation with field observations, Atmos. Environ. 27A (15) (1993) 2265–2285.
[56] A. Venkatram, Model evaluation, in: A Short Course on Air Pollution Modeling, Am. Meteorol. Soc., Boston, MA, 1986.
[57] R.L. Dennis, Issues, design and interpretation of performance evaluations: ensuring the emperor has clothes, in: C. De Wispelaere, F.A. Schiermeier, N.V. Gillani (Eds.), Air Pollution Modeling and Its Applications, Plenum Press, New York, 1985, pp. 411–424.
[58] D.L. Ermak, Field validation of dispersion models for dense-gas releases, in: C. De Wispelaere, F.A. Schiermeier, N.V. Gillani (Eds.), Air Pollution Modeling and Its Applications, Plenum Press, New York, 1988.

[59] M. Hightower, L. Gritzo, A. Luketa-Hanlin, J. Covan, S. Tieszen, G. Wellman, M. Irwin, M. Kaneshige, B. Melof, C. Morrow, Guidance on risk analysis and safety implications of a large liquefied natural gas (LNG) spill over water, Sandia National Laboratory, Sandia Report SAND2004-6258, December 2004.

[60] B. Kosovic, A large Eddy simulation study of a quasi-steady, stably stratified atmospheric boundary layer, J. Atmos. Sci. 57 (2000) 1052–1068.

[61] Wind Tunnel Visualization Study of LNG Vapor Barrier & Obstacle Evaluation (Wind-Tunnel Pre-Field Test), Fluid Mechanics and Wind Engineering Program, Colorado State University, 85-86RNM3, 5-3 6419, 1986.

[62] S.T. Chan, FEM3C: An Improved Three-dimensional Heavy Gas Dispersion Model—User's Manual, UCRL-MA-116567 Rev. 1, Lawrence Livermore National Laboratory, 1994.

[63] S.T. Chan, A Three-dimensional Model for Simulating Atmospheric Dispersion of Heavy-Gases Over Complex Terrain, UCRL-JC-127475, Lawrence Livermore National Laboratory, 1997.